

ANALYSES WITH THE FSTATE CODE:

FUEL PERFORMANCE IN DESTRUCTIVE IN-PILE EXPERIMENTS

T. H. Bauer and C. C. Meek*

Reactor Analysis and Safety Division

Argonne National Laboratory

9700 South Cass Avenue

Argonne, Illinois 60439

DISCLAIMER

This report was prepared as an account of work sponsored by an agency of the United States Government. Neither the United States Government nor any agency thereof, nor any of their employees, makes any warranty, express or implied, or assumes any legal liability or responsibility for the accuracy, completeness, or usefulness of any information, apparatus, product, or process disclosed, or represents that its use would not infringe privately owned rights. Reference herein to any specific commercial product, process, or service by trade name, trademark, name, or otherwise does not necessarily constitute or imply its endorsement, recommendation, or favoring by the United States Government or any agency thereof. The views and opinions of authors expressed herein do not necessarily state or reflect those of the United States Government or any agency thereof.

ABSTRACT

Thermal-mechanical analysis of a fuel pin is an essential part of the evaluation of fuel behavior during hypothetical accident transients. The FSTATE code has been developed to provide this required computational ability in situations lacking azimuthal symmetry about the fuel-pin axis by performing 2-dimensional thermal, mechanical, and fission gas release and redistribution computations for a wide range of possible transient conditions. In this paper recent code developments are described and application is made to in-pile experiments undertaken to study fast-reactor fuel under accident conditions. Three accident simulations, including a fast and slow ramp-rate overpower as well as a loss-of-cooling accident sequence, are used as representative examples, and the interpretation of FSTATE computations relative to experimental observations is made.

I. INTRODUCTION

Thermal-mechanical analysis of a fuel pin is an essential part of the evaluation of fuel behavior during hypothetical accident transients. The goals of such analyses are not only the time and location of a cladding breach, but also information related to material motion prior to and after cladding failure. The FSTATE code has been developed to provide this required computational ability in situations lacking azimuthal symmetry about the fuel-pin axis. This present

paper describes current developments and FSTATE's application to in-pile experiments in the sodium cooled fast reactor program.

The real world environment of an operating fuel pin is seldom axisymmetric. Uncontrollable off-center placement of a fuel pellet or slightly out-of-round cladding can lead to asymmetric fuel temperatures and heat flux [1]. Normal coolant temperature profiles varying radially across pin assemblies provide non-axisymmetric coolant temperature environments to individual

* Present Address: EXXon Production Research Co.
P. O. Box 2189 Houston, Texas 77001

pins. Moreover, under hypothetical accident conditions initial pin failures or partial coolant voiding, in an assembly certainly break any prior circumferential symmetry in the environment of the remaining pins.

Of, perhaps, more immediate interest is the fact that current in-pile experiments, undertaken to study fast reactor fuel behavior under accident conditions, are performed under conditions where both the power generation within a fuel pin and its coolant temperature environment are far from axisymmetric. In transient testing at the thermal Transient Reactor Test Facility (TREAT) reactor [2] neutron flux (and power generation) decreases both as the center of individual pins and as the center of the pin bundle is approached, due to self shielding effects. In a typical seven-pin test bundle power density may vary around the circumference of an edge pin by a factor of two. Sodium coolant temperature variation around this same circumference, while quite small under steady state conditions, may be of order 100 deg-K as computed under severe transient conditions often with regions of coldest sodium adjoining regions of hottest fuel.

It is important to account for the effects of such asymmetry on fuel behavior. Consideration of force balance implies that fuel straining will be averaged azimuthally (roughly). However, fuel pin failure will be governed by the temperature and strain history of the hottest cladding node. Estimation of peak fuel temperatures, melting threshold and fuel vapor pressure will reflect principally the azimuthal slice of peak power generation. To the extent that azimuthal asymmetry is significant, no single axisymmetric or single azimuthal "slice" computation can account for all of these features.

The FSTATE code implements models for transient, non-axisymmetric (r, θ) thermal, fission gas, and mechanical behavior of a single axial fuel pin segment undergoing

an accident transient. Fig. 1 presents the relevant geometry. By treating asymmetries, FSTATE can furnish a capability for analysis in areas where axisymmetric modeling is inappropriate. However, since only one axial segment is considered, FSTATE must rely on other analyses for information, such as coolant temperatures, that couple segments in the axial direction.

The FSTATE code was first reported by C. C. Meek in Ref. [3]. Its two-dimensional heat transfer and fission gas redistribution computations were stringently tested and have not been altered. Further development of FSTATE has been chiefly motivated by its application to in-pile experiments. Significant improvements have been made to the transient mechanics model to insure globally correct force balances across the whole pin cross section. Elastic deformation of fuel is now included and back and forth elastic-plastic transitions in the cladding are now possible. A simple coolant voiding/cladding dryout model has been added which extends FSTATE's usefulness to loss-of-flow (LOF) transients. A variety of auxiliary computations are now available to evaluate pin failure threshold and the potential for post-failure fuel motion.

Another development to the system as a whole has been to link FSTATE to the coolant temperature output of the thermal-hydraulic COBRA [4] code. COBRA computes the fuel's circumferentially varying coolant temperature environment as a function of time and axial position. Successful use of this system in the prediction of pin-failure thresholds in transient overpower (TOP) in-pile experiments has been reported in Ref. [5].

The remainder of the present paper outlines the features and structures of the current FSTATE and describes the new mechanics model, coolant voiding/clad dryout model, and auxiliary computations. The position of FSTATE in current in-pile experiment analyses is outlined. Examples of FSTATE computations

are taken from three types of in-pile experiments: fast TOP's, slow TOP's and LOF's which illustrate the wide variety of transient conditions that may be fruitfully studied with this code. While present application is in the field of in-pile experiments, it must be emphasized that FSTATE has potential application in describing transient fuel pin behavior whenever cooling or power generation lacks azimuthal symmetry.

2. THE FSTATE CODE.

Organization

The FSTATE code models a fuel pin's transient thermal, fission gas redistribution and mechanical performance at a single axial location over a 180° angular slice, as shown in Figure 1. Number of radial and azimuthal nodes, fuel characterization, initial fission gas content, power generation history and coolant temperature history must all be provided as input. As is appropriate to sodium cooled fast reactors, present analyses assume fuel is mixed Pu, U oxide, cladding is 316 SS and coolant is sodium. Material thermal and mechanical properties are taken from the compilation of Liebowitz, et. al., [6] and the Nuclear Systems Materials Handbook [7].

The organization of an FSTATE computation at a given time-step is shown in Figure 2. Arrows on the solid lines indicate flow of information in the computation. Arrows on dashed lines indicate information fed back from the previous time step. Clearly, from Figure 2, the thermal computation acts as the principle driver for the other modules, followed by the fission gas release, swelling and redistribution computations (in problems where significant fission gas is present). Aside from a varying fuel-cladding gap, these "driver" computations employ fixed geometry with fuel densities and porosities unaffected by the mechanical deformation computed later.

As presently constructed, FSTATE

requires modest computer resources. Running FSTATE on the Argonne National Laboratory IBM system needed less than 300 Killobytes of core and several minutes CPU time for each of the examples described in this report (full transient, single axial height).

Thermal Computations

The two-dimensional (r, θ) thermal computation and its validation is described in Ref. [3]. Temperatures in FSTATE are computed for given input coolant temperature boundary conditions, power generation, and initial conditions. Radial and azimuthal conduction are considered, together with an azimuthally varying gap conductance. Energy balances on a given volume element result in a system of finite difference equations. Solution of these equations is obtained via an alternating directions technique [8]. Melting transitions are considered in both fuel and cladding.

A simple coolant voiding/clad dryout model is included in the thermal computation. When the average coolant temperature surrounding the pin exceeds the sodium vaporization temperature at the (input) system pressure, coolant is assumed voided with the exception of a residual film of initial thickness input by the user. Coolant temperature is fixed at its saturation value and further heat flow to the coolant acts to vaporize the film. When the film is vaporized, no further heat is transferred to the coolant. Realizing that the focus of FSTATE is not coolant dynamics, this simple model provides to the user the flexibility to force upon the computation knowledge of voiding obtained elsewhere.

Fission Gas Release, Swellings, and Redistribution Computations

One consequence of asymmetric temperature distributions during accident transients is asymmetric fission gas release, its redistribution and fuel swelling. With a knowledge of thermal conditions in both space and time, estimates of transient fission gas

release, intragranular swelling, and gas redistribution within the fuel porosity can be made. Since fission gas effects have been suggested to be of particular importance to the character of fast reactor accident progression after cladding breach, careful delineation of gas behavior is necessary. The present transient, two-dimensional treatment provides an ability to obtain a detailed view of such behavior. In the present version of FSTATE the user inputs a porosity and permeability for restructured and unrestructured fuel (see Fig. 1). A user input fission gas density initializes fission gas in the unrestructured fuel.

FSTATE incorporates the PFRAS [9] representation of intragranular fission gas release and swelling. The resulting redistribution of fission gas within the fuel porosity is treated via a Darcy flow formalism [10]. Since redistribution is a transport phenomena, it is treated in much the same manner as the temperature. Mass balance on a given volume element result in a series of finite difference equations which are solved using the alternating directions method. Details of the computation are found in Ref. [3]. Once fuel melting begins, gas present both in molten fuel and in the associated interconnected porosity is assumed to move to the available volume in the central cavity.

Calculation of Cavity Pressure

A description of a central cavity that contains molten fuel and gas is important both as an inner pressure boundary for the mechanical computation and as a source term of molten fuel and driving force for studies of fuel motion after cladding breach. In FSTATE all molten fuel, initial cavity gas plus released fission gas occupies a central cavity within a ring of solid fuel and its

size and pressure is adjusted at each time-step. Because FSTATE computes only a single axial slice, no communication exists with either a fuel pin's gas plenum or the central cavity at other axial heights. While the importance of such communication is difficult to assess in general, clearly, peak cavity pressures as computed by FSTATE may be overestimated.

Mechanical Computation

Background information for the transient fuel mechanics analysis may be found in Ref. [3]. The model remains simple in concept. A series of azimuthal wedges of solid fuel and cladding are forced by a plane strain mechanics model to be in equilibrium with each other and a central cavity. If melting has taken place, an azimuthally averaged melt-radius defines the boundary between the solid fuel and the central cavity. The model does account for azimuthal asymmetry, emphasizes global features and takes advantage of important symmetries produced by requirements of equilibrium.

FSTATE assumes half-plane; e.g., $\theta - \theta$ symmetry in its thermal and fission gas driver computations. In addition, equilibrium requires that forces diagonally opposite; i.e., at " θ " and " $\pi + \theta$ " balance. Thus, in the halfplane ($0 < \theta < \pi$) FSTATE computation forces must be symmetric about " $\pi/2$ ". When the fuel and cladding are in contact, this symmetry is maintained by averaging the unrestrained thermal and fission gas swellings at angle " θ " with that computed at " $\pi - \theta$ ". Since it is these fuel swellings which drive the mechanics computation, an appropriate, whole pin, mechanical equilibrium is assured.

Clad yielding is treated by restricting clad stress to within a yield surface dependent upon azimuthal peak temperature, strain rate, and accumulated plastic strain [11]. Back and forth transitions between elastic and plastic cladding are permitted. Elastic constants of solid fuel depend on the input porosity and number of cracks. The latter correlation is taken from the LIFE fast reactor, fuel performance code¹ [12] and

¹The fuel's Young's modulus and Poisson's ratio are multiplied by factors; $(2/3)^N$ and $(1/2)^N$ is the number of radial cracks.

is very important in determining the fuel's strength. In FSTATE the user may explore the range of possibility from "strong" to "weak" fuel simply by varying the number of input cracks. FSTATE incorporates no cracking, crack healing or plastic yield (creep) modeling in the fuel so these parameters are left to user input.

Auxiliary Computations

As indicated in Figure 2, present FSTATE incorporates auxiliary computations to "predict" cladding failure and estimate an adiabatic work potential for fuel motion post-failure. These computations are termed auxiliary in that their results do not influence other modules in FSTATE. Thus, FSTATE computations may continue in time as long as computations with intact geometry are deemed useful. This time period may extend well beyond the time when cladding has failed and terminate only when significant fuel has moved.

Cladding failure is modeled via a damage integral formulation using the Larson-Miller parameter [14] on the basis of the cladding stress, temperature history. The correlation presently used is one for unirradiated cladding. Transient damage accumulation is calculated for each azimuthal segment. By so doing, the location of failure on the pins periphery may be determined.

An independent correlation for cladding unrecoverable, transient, plastic strain developed for use in fast reactor fuel performance codes of the United Kingdom (UK) [13] has also been incorporated into FSTATE. Plastic strain is here correlated to the cavity pressure and clad temperature history, and failure

is predicted when this quantity is ~2%. Azimuthally, the hottest cladding node will always fail first.

The two cladding failure correlations tend, in practice, to compliment one another. In situations where fuel is strong, cavity pressure low and differential strain stresses the cladding, the Larsen-Miller approach is most relevant. On the other hand where fuel is cracked (weak), so that the cladding is not stressed until cavity pressure increases, the UK plastic strain correlation is useful, even when such pressures increase without bound. Under these latter circumstances, when FSTATE no longer computes a force balance, the Larsen-Miller correlation no longer receives correct input, and the transient plastic strain correlation must be relied upon.

The computation of adiabatic work potential is a device using an intact geometry calculation, for anticipating fuel motion once the fuel pin has failed. Specifically, these are straightforward thermodynamic computations of the amount of work (per unit mass of fuel) that could be performed in an adiabatic expansion of fuel, cavity and intergranular gas or fuel vaporization out to the ambient channel pressure. Work potentials provide a common basis for quantitatively ranking the various fuel dispersion mechanisms in a test. (Work potentials from other dispersive mechanisms such as steel vaporization and sodium vaporization must be estimated by other means.) These computations are most useful at and beyond the time of cladding breach.

3. ANALYSIS OF DESTRUCTIVE IN-PILE EXPERIMENTS

General Features

In addition to the previously discussed, non-prototypic, power generation and coolant temperature asymmetry, in-pile experiments also suffer from severe limitations on data that may be obtained during a test. The safety requirement that all tested reactor materials be isolated under any conceivable circumstance serves, in general, to insulate the experimenter from the experiment. The upshot is great reliance upon calculations to supplement the relatively fragmented description of the test environment obtainable from test instrumentation and post-test disassembly.

To be more specific present discussion will concern 3 and 7-pin core-disruptive accident simulations in a flowing sodium environment performed in the TREAT reactor. Ref. [2] provides good background information. Information related to fuel performance during these tests is sparse. Thermocouples monitor coolant temperature above and below the test bundle. Information about fuel pin failure and coolant voiding is obtained from flowmeters and pressure transducers placed above and below the test bundle. In the test bundle itself the only instrumentation is, typically, thermocouples which monitor the temperature on the outer surface of a, usually thin, duct wall surrounding the pin bundle. Once fuel begins to move the fast neutron hodoscope [15] at TREAT can monitor changes in its distribution by detecting fast neutrons from the tested fuel above the thermal reactor background radiation. (Fast neutrons, fortunately, escape the test vehicle containing the experiment.) Broadly speaking, the role played by FSTATE (or other fuel performance codes) in test analysis is the following: Computed thermal and mechanical conditions allow the quality of the accident simulation to be theoretically assessed prior to fuel disruption, and, after disruption, aid in

assessing the significance of the material motions observed.

Use and Validation of FSTATE in Test Analysis

As discussed in Sec. 2., FSTATE requires, as input, the coolant temperature history of the fuel pin's environment, fuel characterization information - if irradiated, as well as the driving power and coolant flow transients to which the fuel is subjected.

Typically coolant temperatures in the small test bundles are computed with the COBRA code.[4]. The COBRA thermal-hydraulic code is a valuable tool in situations such as TREAT simulation where power generation asymmetries are important. A test bundle cross section is explicitly modeled by subdivision into coolant subchannels pin sectors, and duct wall sectors. Measured pin-to-pin and pin-internal power generation asymmetries, radial and azimuthal are taken into account. Coolant temperature asymmetries across the test bundle are computed. Heat losses to and beyond the duct wall are also accounted for. In test analysis a reasonable agreement must exist between the measured inlet and outlet coolant temperatures, measured temperature on the bundle's duct wall, and the COBRA calculations. COBRA calculated coolant temperatures of subchannels which neighbor the fuel pin of interest are then used as input to FSTATE.

Fuel characterization information concerning pre-irradiated fuel is obtained from several sources. The most desirable is from destructive examination of a "sibling" pin that had undergone a similar irradiation history. Failing this, or to supplement sparse experimental data, fuel performance codes, such as LIFE-3 [16, 17], provide required information.

Driving functions, such as pin power (including asymmetries) and coolant flowrate, are taken from experiment. These input are consistent with that input to the COBRA code.

In general, FSTATE computes aspects of fuel thermal and mechanical behavior which are not experimentally measured; so experimental validation of FSTATE under test conditions is ambiguous. Nonetheless, the credibility of FSTATE computations may be experimentally assessed in three ways. First, a comparison of experimental indications of pin failure with the Larsen-Miller and UK plastic strain failure threshold computations can be made. Second, if the experiment gives a clear indication of the axial location of failure, comparison with the FSTATE failure threshold computation can be made. Finally, the nature of the observed post failure fuel motion may be qualitatively compared with the pin conditions as computed by FSTATE, specifically the adiabatic work potentials.

ANL-TREAT Tests E8, H6 and L7

Test analysis with the FSTATE code is here illustrated with results from three small bundle experiments performed by Argonne National Laboratory on the TREAT reactor testing pre-irradiated fuel in flowing sodium. Test E8 [18] is a 7-pin simulation of a 3-5 \$/s TOP accident. Test H6 [19] was also a 7-pin TOP accident simulation, but at a significantly slower ramp rate (.50 \$/s). Test L7 [20] was a 3-pin simulation of a LOF-TOP with an event sequence of: sodium flow coastdown, coolant voiding, followed by a power burst to about 20 times that of the fuel's nominal power rating. Tests E8 and H6 used "short" fuel pins of active fuel length 340 mm whereas test L7 used fuel of more prototypic length 880 mm. In all three tests fuel was pre-irradiated to bring about prototypic fuel restructuring and significant fission gas content. Miscellaneous information regarding test fuel and conditions is given in Table I.

In all three cases significant power skewing existed across the test bundle and within the individual test pins. In tests E8 and H6 attention is focused on the edge pin of highest power rating for which there is a radial power depression of

about 1.7: 1 between the pin surface, azimuthally averaged, and center. Additionally, around the pins circumference, itself, power varies with a maximum to minimum ratio of ~1.7. The edge pin peak power is generated at the surface facing outward, away from the pin bundle center. In test L7 all three pins had roughly the same power rating. The radial power depression is here about 2.3: 1 between the pin surface, azimuthally averaged, and center, but the power variation around the pin circumference is about the same magnitude and reflects the same orientation as in tests E8 and H6. These power generation asymmetries are explicitly modeled in the FSTATE computations.

The coolant temperature environment of these pins, as computed by COBRA, reflects not only the power skewing as described, but also details of the coolant flow geometry. In the E8 test peak coolant temperature are circumferentially oriented to directions midway between pin bundle center and bundle edge with a computed azimuthal variation of ~ 45 deg-K at the top of the fuel at the time of observed first pin failure. On the other hand in test H6 peak coolant temperatures are circumferentially oriented toward the bundle center with a computed azimuthal variation of ~ 50 deg-K at the top of the fuel at the time of the first observed pin failure. In test L7 peak coolant temperatures are also oriented towards the bundle center, with a computed azimuthal variation of ~115 deg-K at the top of the fuel at the time of observed coolant voiding.

FSTATE Analyses of Tests E8, H6 and L7

In all three tests limited sibling pin information was available to characterize the fuel. In the case of L7 sibling pin information was sufficient to provide the needed input data. In the cases of H6 and E8 fuel restructuring in sibling pins did not produce an easily measured central cavity, as required by the code, so LIFE-3 computations were used to determine the

axial distribution of central cavity radius as well as axial and radial distributions of porosity. These computations account for fuel mass distribution in a credible way. Also, in H6 and E8, LIFE-3 computed axial and radial distributions of retained fission gas were used. These were consistent with over all fission gas retention in the sibling pin. Initial fuel-cladding gaps were in all cases estimated from sibling pin data. Based on sibling pin examination, the fuel in all three tests was assumed to be very weakened by cracking at the start of the tests.

The COBRA calculations which were used to compute the coolant temperature environment for the fuel pins of interest assumed only single phase flow. The FSTATE coolant voiding model was invoked at the time when the inlet flowmeter experimentally indicated flow reversal. (In studies of failure threshold in tests E8 and H6, this procedure was bypassed so as not to prejudice the outcome, since coolant voiding follows fuel pin failure in these cases.) In all computations the driving functions of power and flow were taken to be the nominal values for the hottest pin in the cluster at the appropriate axial height.

Failure threshold in tests E8 and H6 was computed by FSTATE to occur as a result of a rapidly increasing pin internal (cavity) pressure. (The UK plastic strain criterion was used.) Axially, failure is computed to occur nearly simultaneously in the quarter of the fuel just above the midplane in test E8. In test H6, it is computed to occur at the midplane. Circumferentially, cladding breach occurs at the hottest azimuthal node. For test E8, this is computed to be toward the bundle edge while, for test H6, it is toward the bundle center. A failure threshold study was not done for test L7, since the mechanism of cladding breach was presumably melting not straining.

These nominal computations seem to be in reasonable agreement with available

experimental data. The computed timing of cladding failure in these nominal calculations is about 10 ms late in test, E8 and about 120 ms early in test, H6. Considering the full width at half maximum of the power bursts in tests E8 and H6 are about .5 s and 1.5 s respectively, these discrepancies are quite small. Axially, indications from the fast neutron hodoscope and loop sensors as to where pin failure first occurred also seem in reasonable agreement with FSTATE predictions.

Caution should be exercised in evaluating agreement of these nominal calculations with experiment. While experimental indications of the time of cladding failure in tests E8 and H6 are probably significant to the millisecond range, experimental information concerning the axial location of failure is very qualitative [18, 19]. In most TREAT experiments of this type a systematic 6-10% error in nominal pin-power generation is possible [21, 22]. Moreover, the E8 and H6 test fuel underwent minimal restructuring, and the computed failure times at any axial position is very sensitive to the imperfectly known input central cavity size and the porosity in the adjoining fuel. Uncertainties in the calculated time of cladding failure can then be estimated as $\sim \pm 30$ ms in test E8 and $\sim \pm 100$ ms in test, H6. (This uncertainty is in addition to any systematic effect introduced by "imperfections" in FSTATE's modeling schemes.) The present nominal calculations while consistent with existing data around the failure threshold, should not be regarded as quantitatively definitive, but rather illustrative of fuel conditions in these experiments.

Selected results of the FSTATE analyses of tests E8, H6, and L7 are shown in Figs. (3-11). Times shown in the Figures (3-11) are actual test times used in Refs. [18-20].

Figures 3-5 illustrate thermal conditions of

interest at the midplane of the hottest pins in the bundle in the three tests studied. Figures 3 and 4 show isotherms at melting onset for tests E8 and H6 and the subsequent advance of the melt front (solidus). Power skewing in the pin leads to off-center melting that is far more serious for high ramp rates (E8) than for low (H6). Without power skewing melting would originate at the pin center and propagate radially outward. The coolant temperature environment of the pin at melting onset is shown on the periphery of the pin. Figure 5 shows temperature profiles in test L7 at the end of the power flattop, just before coolant voiding and 0.5 sec. later at peak power, just before vigorous fuel motion was observed by the hodoscope. The coolant temperature environment is indicated on the pin periphery. At peak power the effect of power skewing is quite striking and maximum fuel temperatures approach that where vapor pressure might be important, as discussed below.

Figures 6 and 7 show computed pin-internal (cavity) pressures and cladding hoop stress in the hottest azimuthal cladding node, at the axial midplane of the hottest pin, for overpower tests E8 and H6. Cavity pressure increases abruptly with melting: cavity volume decreases and fission gas is released to the cavity. Fuel vapor does not contribute significantly to the pressure shown. The effect of fuel strength is shown for illustration in Fig. 6 by computations of cladding hoop stress with different numbers of input cracks. The cracking parameter variations have minimal effect on the cavity pressure history. Moreover, in the present examples, variation of the cracking parameter significantly influences the hoop stress only before the rapid rise of central cavity pressure. As stated earlier, nominal computations assume fuel in a cracked, weakened state. Given FSTATE's assumptions of plane strain and no central cavity pressure communication, the reader should view these curves with caution.

While it is apparent that fission gas plays a significant role in producing

computed pin failures, its role in producing subsequent fuel motion is less certain. Figures 8-11 show computations of the adiabatic work potentials, as described in Sec. 2. Computations are carried out past the point of fuel failure assuming the original geometry intact. In these figures the relative contributions of fission gas and fuel vapor is differentiated.

Figure 8 indicates that, while fuel vapor may not dominate the pin pressure computation of Fig. 6, it does overwhelm inert gas expansion as a dispersive mechanism later in the transient when fuel was in fact observed to move vigorously. Fuel vaporization and expansion simply provides a much more efficient means of converting heat into mechanical work than does heating and expanding an inert gas. On the other hand Fig. 9 shows work potential contribution only from fission gas in test H6. Fuel motion in test H6 is significantly less vigorous [18, 19].

Other dispersive mechanisms such as steel vaporization and sodium vaporization could play a role in tests E8 and H6 but are not as readily estimated from calculations with intact geometry. However, the work potential from steel vaporization may be conservatively overestimated to be ~ 2 kJ/kg (assuming complete mixing of fuel and steel with varying steel fractions). Work potential from coolant vaporization is most readily analyzed by post-test coolant slug-ejection data, and experience from past TREAT test data indicates specific work potentials from sodium slug ejection to be $\sim 1-2$ kJ/kg [23]. Thus, in test E8, fuel vaporization appears to be a likely mode of post-failure fuel dispersion.

Figures 10 and 11 show work potential in test L7, at the midplane of the hottest pin and axially for the hottest pin for various times after the onset of fuel motion. Because the coolant was apparently voided before fuel melted and moved, sodium vaporization does not play a role. It is quite clear from these figures that fuel vapor dominates the

computed work potential in the time domain of fuel motion.

FSTATE computations may overestimate the work potential of fuel vapor. Any fuel relocation that does occur will tend to cause mass mixing, reduce thermal gradients in the fuel, and, hence, reduce the amount of fuel over the vaporization temperature. In the calculations for both tests E8 and L7 complete mixing of molten fuel would eliminate fuel vapor as a contributor to fuel dispersion. Once fuel motion begins, the truth lies, most probably, somewhere between the complete mixing concept and FSTATE intact geometry computation.

4. CONCLUSIONS

The FSTATE Code has been used successfully to analyze fuel behavior in a wide variety of destructive in-pile experiments that simulate overpower as well as loss-of-flow accidents in sodium cooled fast reactors. Although absence of direct measurement of computed quantities make validation difficult, modules incorporated in FSTATE have been developed and tested separately [3], and the illustrative computations presented in Sec. 3 are credible and consistent with existing data.

Deficiencies in the present version of FSTATE stem from the simplicity of its approach. Foremost is the absence of any axial communication of central cavity pressure either with other axial segments or with a pin gas plenum. Additionally, the fuel mechanics treatment is a simple plane strain model. Axial expansion is not permitted. Plastic relief of stress in the fuel (creep) is not considered, nor is a cracking model incorporated (although properties of cracked fuel are considered). These simplifications should be regarded as a trade-off for FSTATE's full, 2-dimensional analytical capabilities. It should be noted that the virtue of including more sophisticated models and calculations in experiment analysis is not readily apparent in comparison with data.

FSTATE can play an important role in accident simulation planning and interpretation. For example, a next step in an analysis could be to use FSTATE to evaluate the quality of the accident simulation, e.g. test E8, H6, or L7, relative to a reference, hypothetical accident in a fast reactor. Effects of power skewing, off-center melting etc. in the simulation may be explicitly studied by comparison FSTATE calculations using the reference, fast reactor conditions. Effects studied could include not only temperature, fission gas behavior and pin failure threshold but also post-failure fuel motion using adiabatic work potential as an approximate figure of merit.

REFERENCES

1. O. McNary and T. H. Bauer, "The Effect of Asymmetric Fuel-Clad Gap Conductance on Fuel Pin Thermal Performance," Nucl. Eng. Des. 63, p. 39 (1981).
2. C. E. Dickerman et. al., "Status and Summary of TREAT In-Pile Experiments on LMFBF Response to Hypothetical Core Disruptive Accidents," Symp. Thermal and Hydraulic Aspects of Nuclear Reactor Safety, Vol. 2: Liquid Metal Fast Breeder Reactors, Atlanta, Ga., 1977, p. 19, O. C. Jore and S. G. Bankoff, Eds., American Society of Mechanical Engineers (1978).
3. C. C. Meek, "The FSTATE Code," ANL-78-72, Argonne National Laboratory, (August 1978).
4. W. W. Marr, "COBRA-3M: A Digital Computer Code for Analyzing Thermal-Hydraulic Behavior in Pin Bundles," ANL-81-31, Argonne National Laboratory (March 1975) also, Nucl. Eng. Des., 53, p. 223 (1979).

5. A. E. Klickman et. al., "Methods of Predicting Fuel Failure-Development and Evaluation," Proceedings of the International Meeting on Fast Reactor Safety and Technology, Seattle Wa., 1979, p. 944, American Nuclear Society.
6. L. Liebowitz et. al., "Properties for LMFBR Safety Analysis," ANL-CEN-RSD-76-1, Argonne National Laboratory (1976).
7. Nuclear Systems Material Handbook, Hanford Engineering Development Laboratory.
8. D. W. Peaceman and H. H. Rachford, Jr., The Numerical Solution of Parabolic and Elliptic Differential Equations, J. Soc. Indust. Appl. Math., 3 28-41 (1955).
9. E. E. Gruber, "A Generalized Parameteric Model for Transient Gas Release and Swelling on Oxide Fuels", ANL-77-2, Argonne National Laboratory (January 1977).
10. J. R. Hoffman and C. C. Meek, Internal Pressurization and Fission-Gas Redistribution in Solid Mixed-Oxide Fuel, Nuc. Sci. Engr., 64, 1-10 (1977).
11. J. M. Kramer, R. J. DiMelfi and T. H. Hughes, "New Method of Calculating Elastic-plastic Behavior of Fuel-pin Cladding," ANL-RDP-68, p. 6.22, Argonne National Laboratory (February 1978).
12. V. Z. Jankus and R. W. Weeks, Nucl. Eng. Des, 18, p. 83, 1972.
13. T. P. Moorhead, "Clad Strain and Melthrough Fracture Mode Analysis for Fast Running Application," Workshop on Predictive Analysis of Material Dynamics in LMFBR Safety Experiments, LA-7938-C, Los Alamos National Laboratory (July 1979); D. J. Hill, private communication, April 1981.
14. J. L. Straalsund et. al., "Correlation of Transient Test Data with Conventional Mechanical Properties Data," Nucl. Tech., 25, p.531 (1975).
15. A. DeVolpi et. al., "Fast-Neutron Hodoscope at TREAT: Methods for Quantitative Determination of Fuel Dispersal," Nucl. Tech., 56, p. 141 (1982).
16. V. F. Jankus and R. W. Weeks, "Life-II-A computer Analysis of Fast-reactor Fuel-element Behavior as a Function of Reactor Operating History," SMIRT-1, Berlin (West), Germany, September 20-24, 1971.
17. M. C. Billone et. al., "The LIFE-III Fuel-element Performance Code," ERDA-77-56, July 15, 1977.
18. R. Simms et. al., "Transient-Overpower Test E8 on FFTF-type Low-power-irradiated Fuel," ANL-77-93, Argonne National Laboratory (1977); R. Simms et. al., Nucl. Tech. 50, p. 225 (1980).
19. R. J. Page et. al., "TREAT Test H6-A 50 cent/s Transient Overpower Accident Simulation," Nucl. Tech. 45, p. 249 (1979).
20. R. Simms et. al., "TREAT Test L7 Simulating an LMFBR Loss-of-Flow Accident with FTR-type Fuel," ANL-80-112, Argonne National Laboratory (1980); R. Simms et. al., Nucl. Tech. 52, p. 331 (1981).
21. R. G. Palm, "Uncertainty of Test Fuel Power Generation in TREAT," Trans. Am. Nucl. Soc. 22, p. 658 (1975).
22. R. Simms, "Calibration Factors for TREAT L-Series Tests L6, L7 and L8," ANL-80-10, Argonne National Laboratory (1980).
23. R. C. Doerner, T. H. Bauer and A. E. Wright, "In-Pile MFCI Test of Carbide Fuel, TREAT Test AX1," Trans. Am. Nucl. Soc. 34, p. 550 (June 1980).

Table I Capsule Descriptions of Tests E8, H6 and L7

<u>Test</u>	<u>Simulation</u>	<u># pins</u>	<u>pre-test irradiation history</u>
E8	3-5 \$/s transient overpower	7	27 kw/m to 5.0 A% burnup in the Experimental Breeder Reactor-II
H6	.5 \$/s transient overpower	7	27 kw/m to 6.0 A% burnup in the Experimental Breeder Reactor-II
L7	loss-of-flow plus power burst to 20x nominal	3	36 kw/m to 3.0 A% burnup in the General Electric Test Reactor

<u>Test</u>	<u>Flattop</u>	<u>burst</u>	<u>Flow (before Failure)</u>	<u>onset of fuel failure</u>
E8	45 kw/m from 4.5 to 6.6 s	to 1024 kw/m at 7.28 s	70 g/s-pin	~ 7.22s
H6	39 kw/m from 4.2 to 6.3 s	to 249 kw/m at 9.29 s	117 g/s-pin	~ 8.92 s
L7	37 kw/m from 4.6 - 13.7 s	to 841 kw/m at 14.19 s	48 g/s-pin, coastdown started at 8.66 s with zero pumping at 16.22 s	~ 13.7 s - coolant boiling ~ 14.25 - Fuel motion

Note: Power history of each test consists of a flattop power plateau followed by a controlled burst. Conditions quoted refer to the midplane of the hottest pin in the test. All information is taken from refs. [18-20].

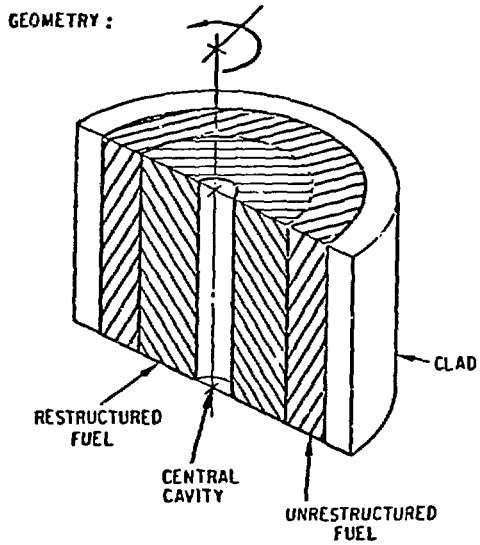


Fig. 1. FSTATE Fuel Pin Geometry

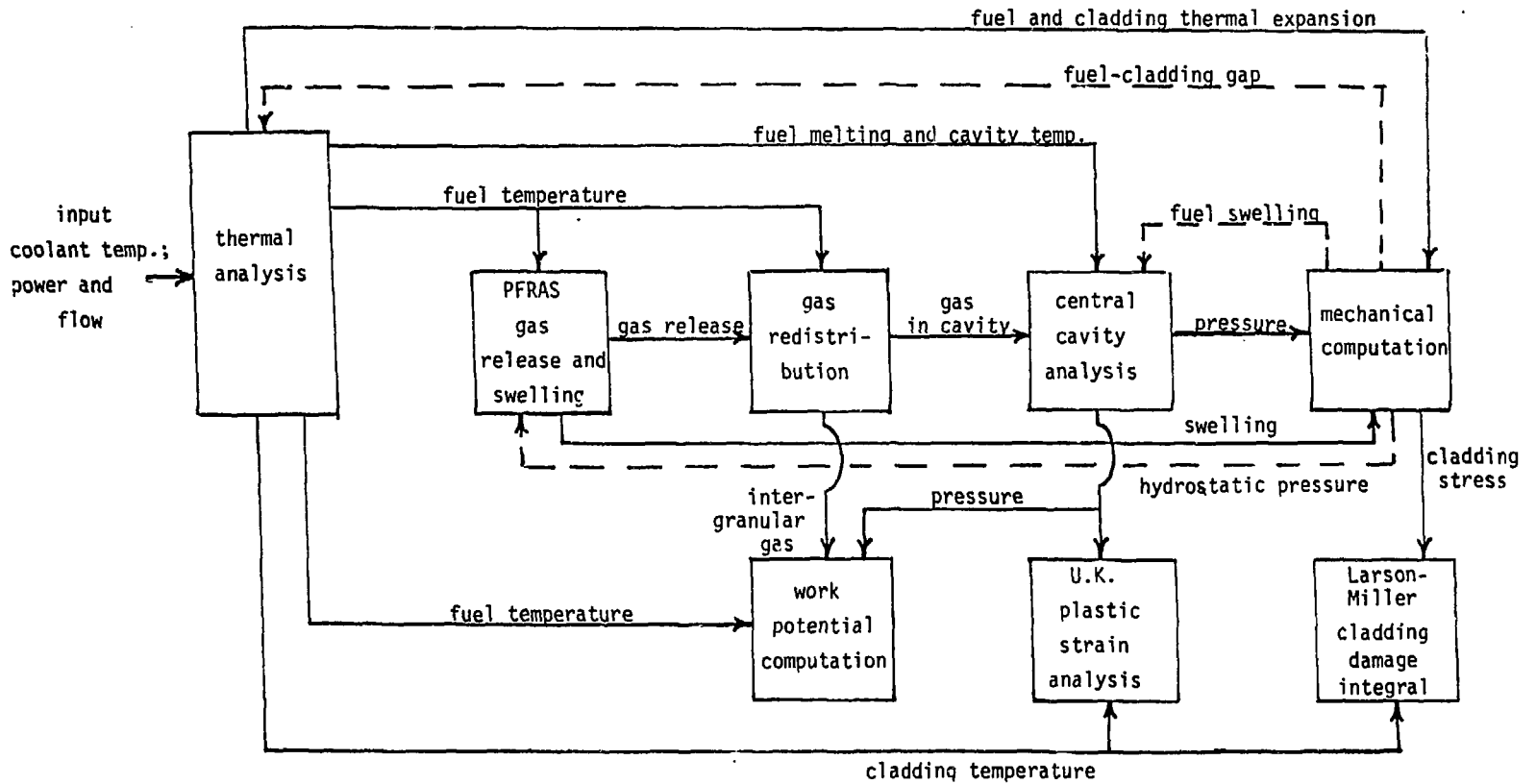


Fig. 2. FSTATE Computation: Logical Flow

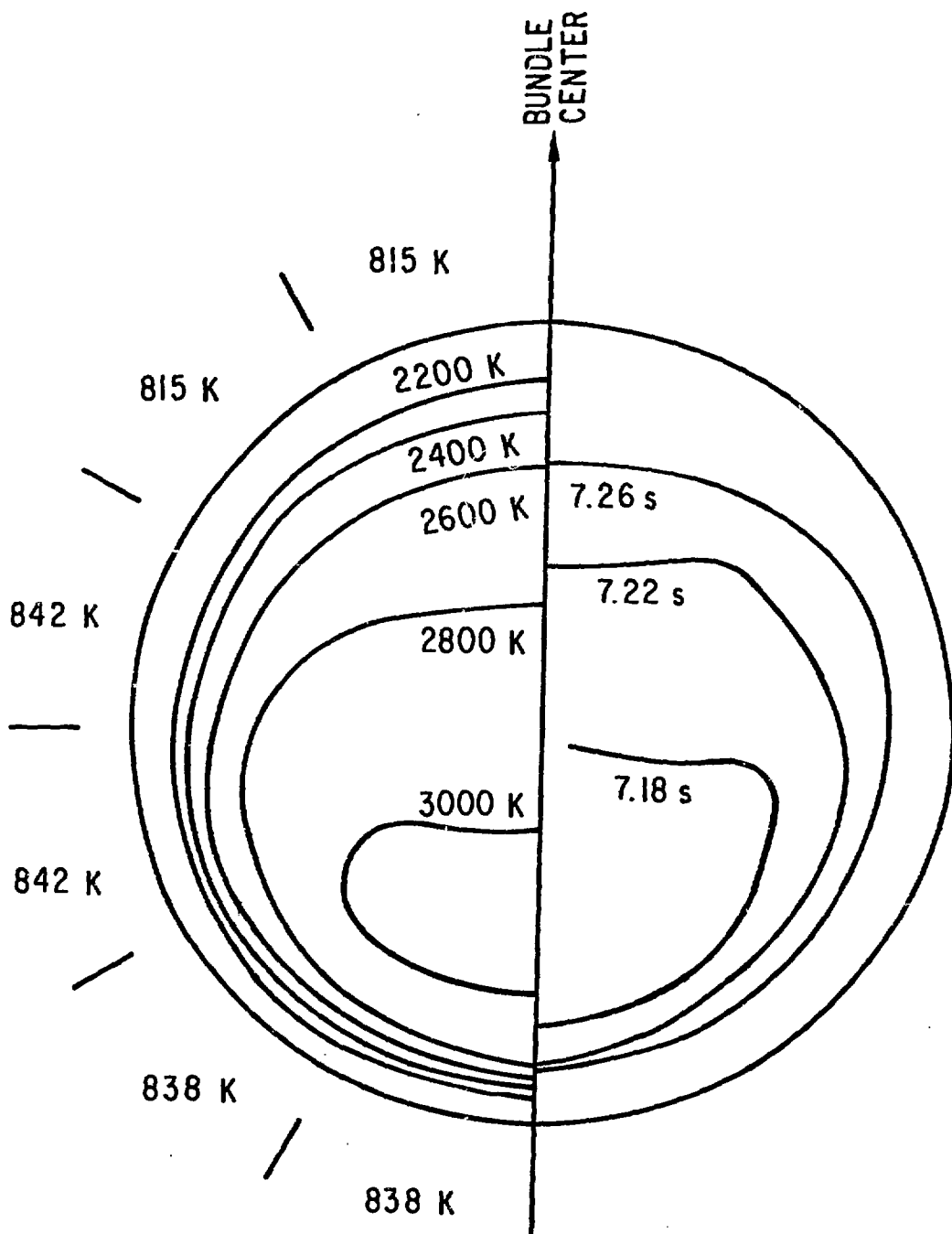


Fig. 3. Test E8: Thermal Conditions at the Midplane of the Hottest Edge Pin.
 Left: Isotherms at Incipient Melting (7.16 s)
 Right: Subsequent Advance of Melt Front

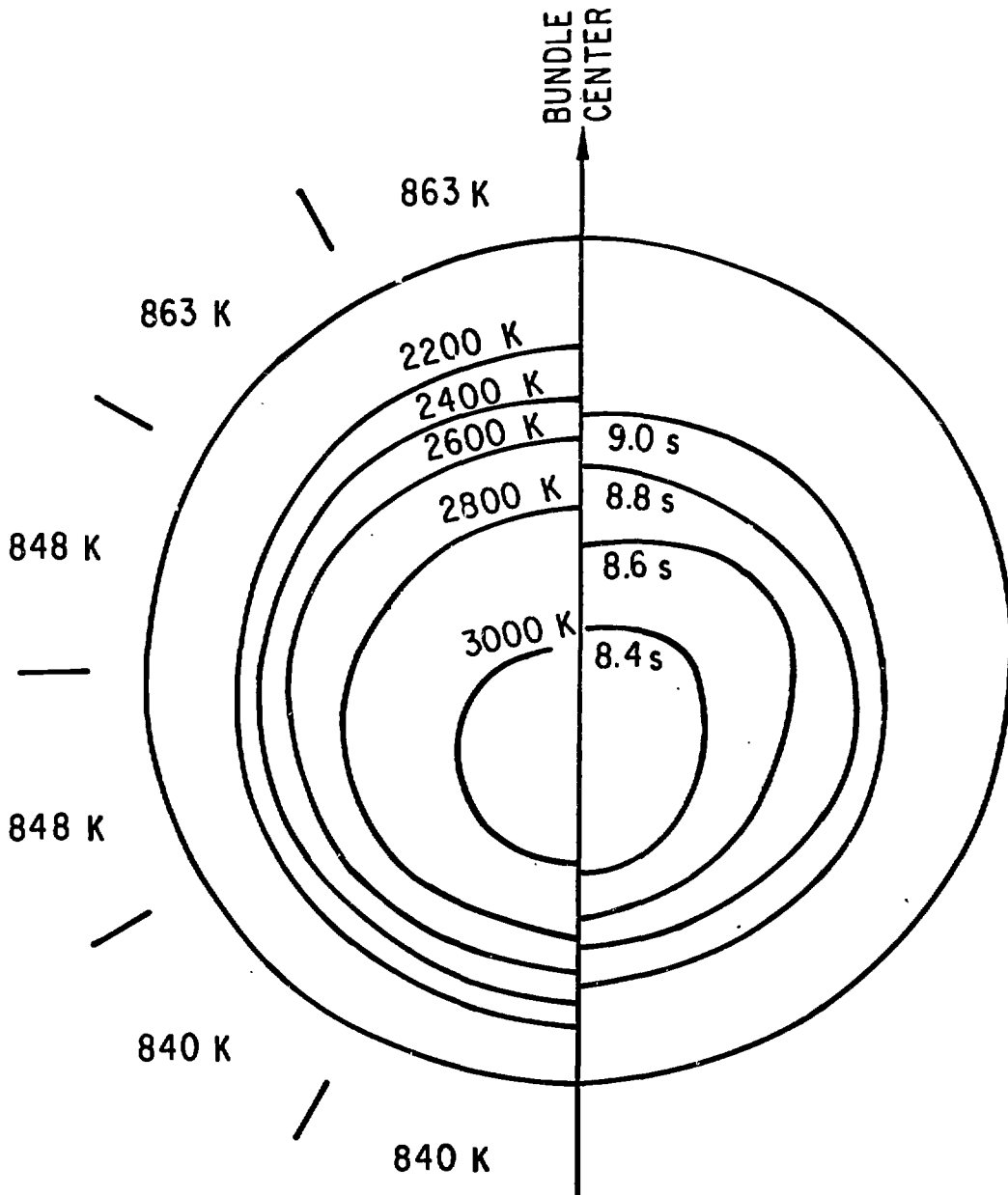


Fig. 4. Test H6: Thermal Conditions at the Midplane of the Hottest Edge Pin.
 Left: Isotherms at Incipient Melting (6.23 s)
 Right: Subsequent Advance of Melt Front

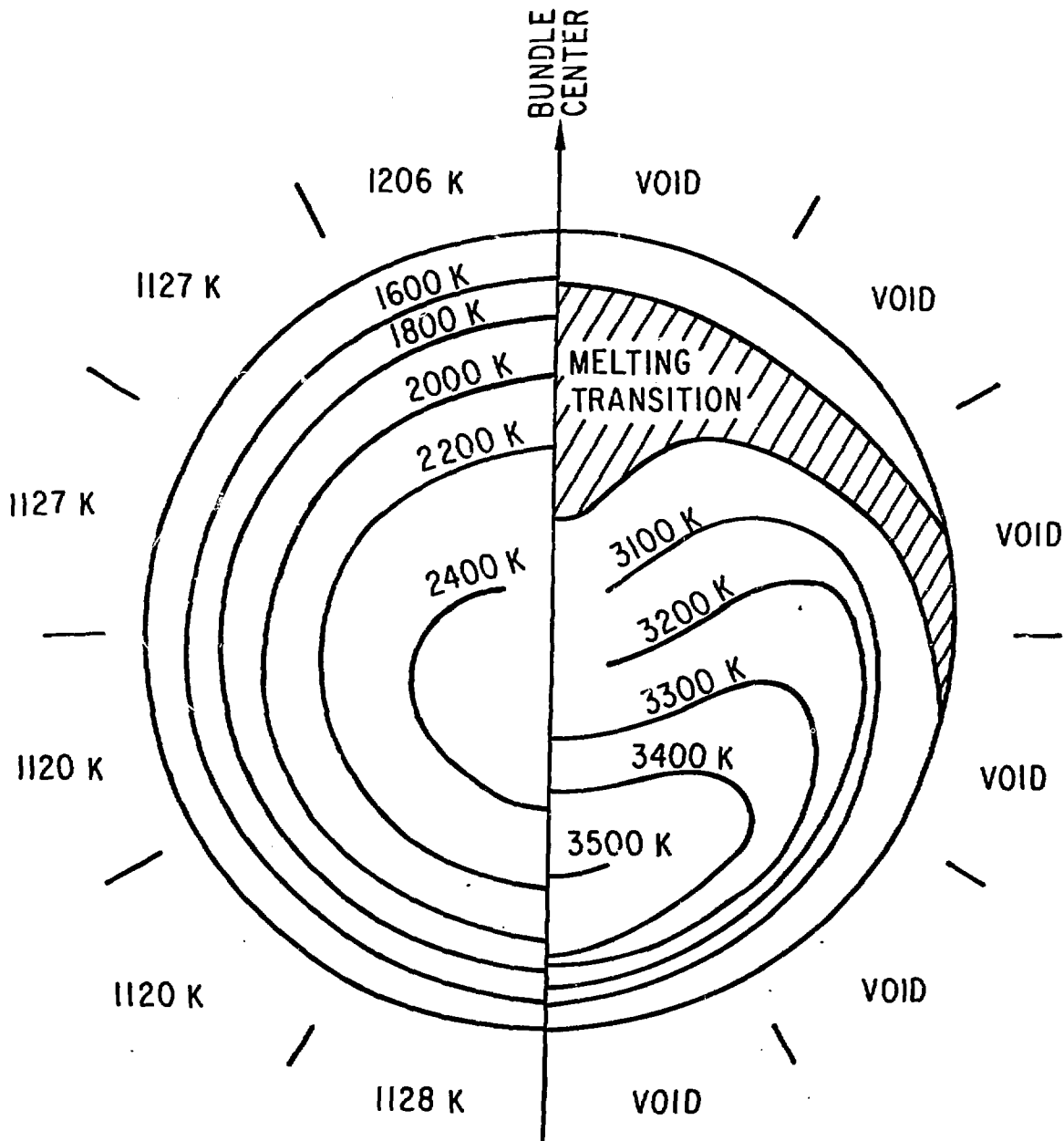


Fig. 5. Test L7: Midplane Fuel Temperatures

Left: Before Burst at Onset of Coolant Boiling
(13.7 s)

Right: Peak Power at Onset of Fuel Motion
(14.2 s)

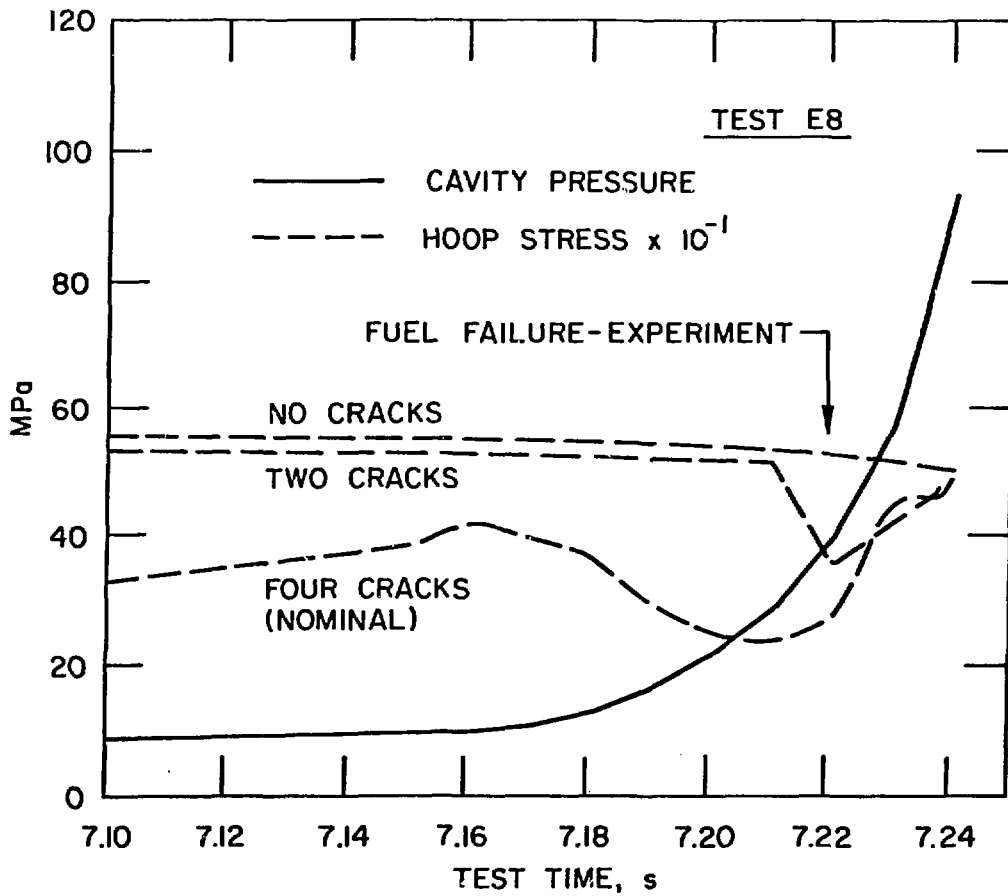


Fig. 6. Midplane Cavity Pressure and Cladding Hoop Stress in Test E8.

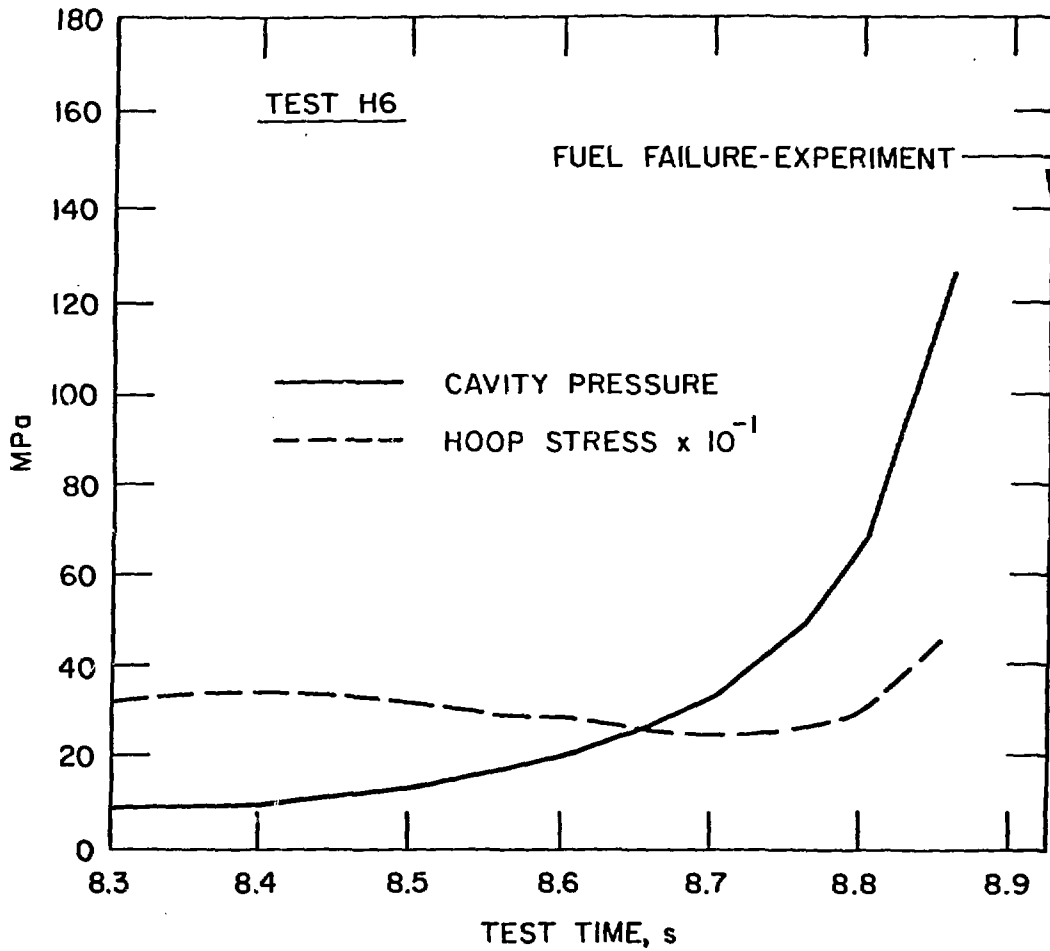


Fig. 7. Midplane Cavity Pressure and Cladding Hoop Stress in Test H6.

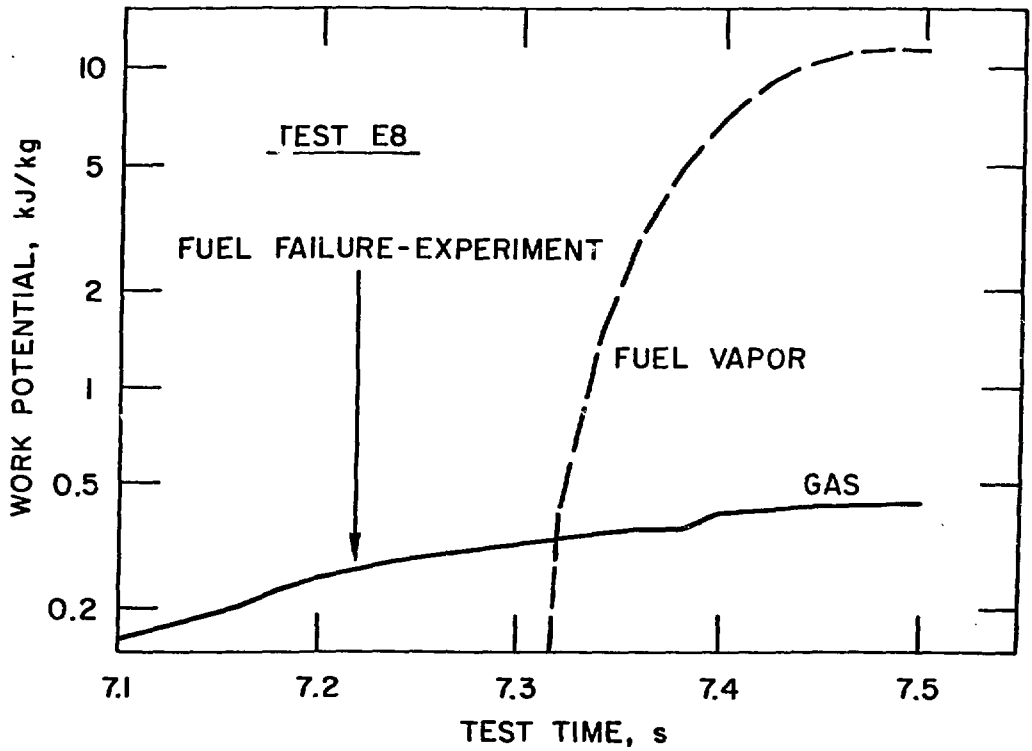


Fig. 8. Midplane Work Potential in Test E8

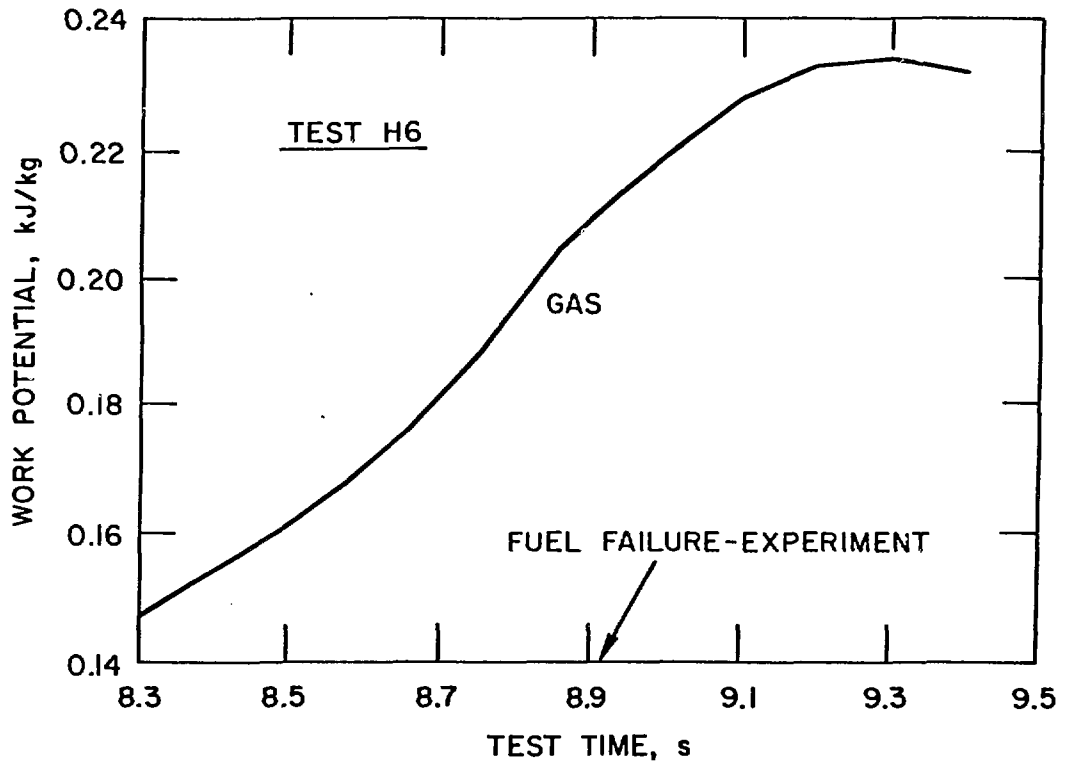


Fig. 9. Midplane Work Potential in Test H6

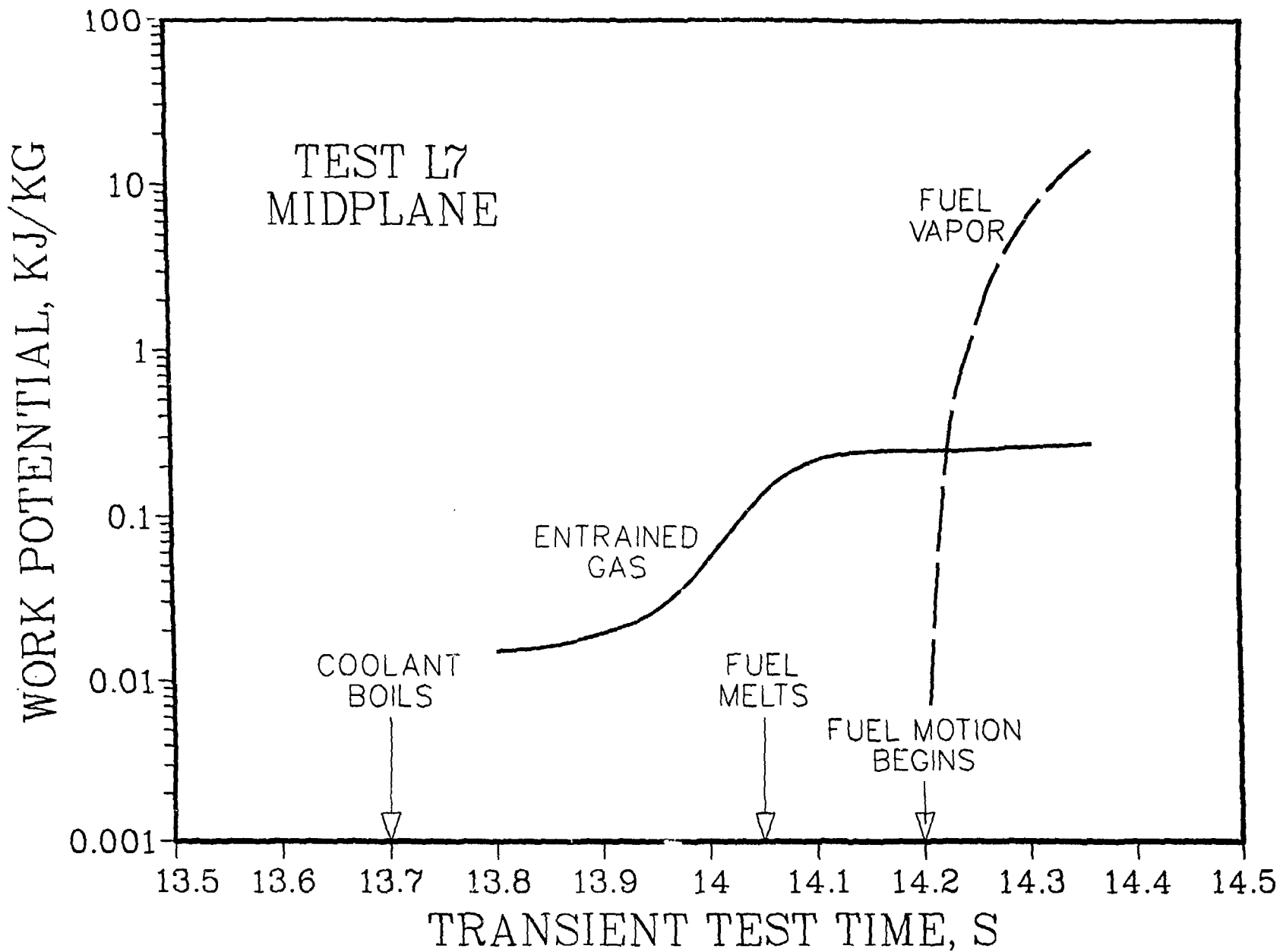


Fig. 10. Midplane Work Potential in Test L7

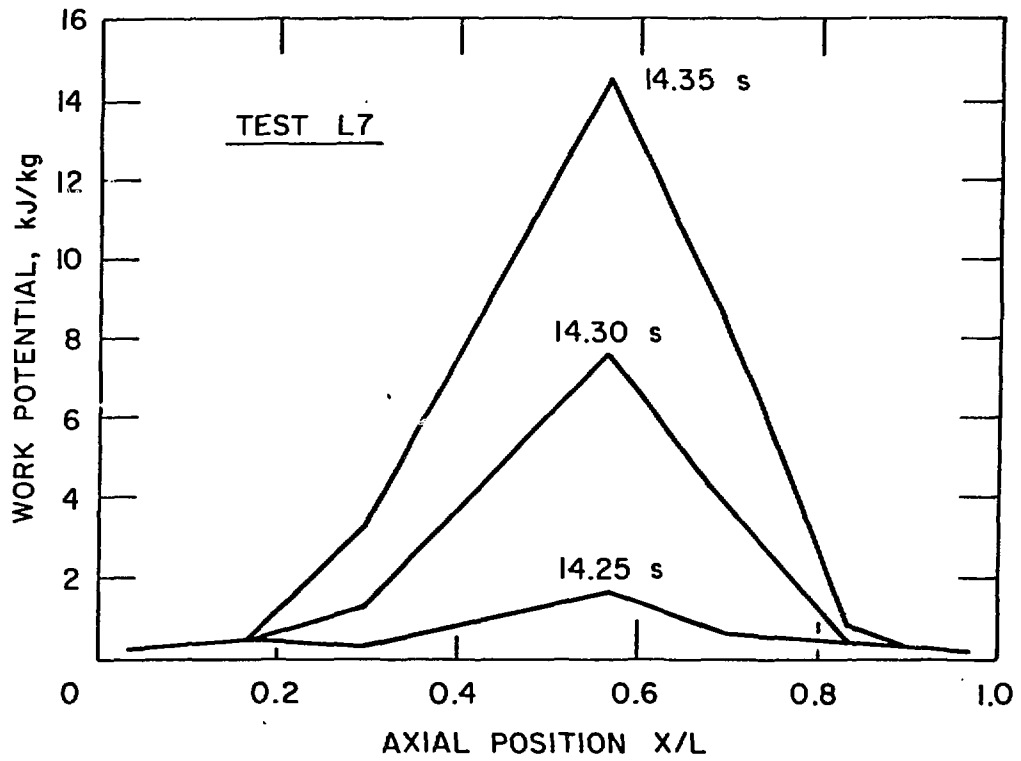


Fig. 11. Work Potential in Test L7 After Fuel Failure: Axial Dependence